MEGA: A LARGE-SCALE MOLECULAR EDITING DATASET FOR GUIDED-ACTION OPTIMIZATION

Anonymous authors
Paper under double-blind review

ABSTRACT

Large language models show strong potential for molecular editing, but progress has been constrained by the limited scale and quality of available training data. To address this, we introduce MEGA, a family of large-scale datasets comprising 31M molecule pairs, each representing a single property-improving chemical edit annotated with an explicit action: *Replace*, *Insert*, or *Delete*. We demonstrate MEGA's utility in a controlled supervised fine-tuning (SFT) setting, where a model trained on MEGA outperforms models trained on existing datasets by up to +21.47 percentage points in hit ratio. Furthermore, we show that Group Relative Policy Optimization (GRPO) post-training with a similarity-aware reward achieves state-of-the-art performance and a remarkable $\sim 36\times$ improvement in data efficiency, while also preserving edit locality. We release MEGA in open access to the community to enable data-centric benchmarks and accelerate progress in molecular editing with generative models.

1 INTRODUCTION

Molecular optimization is critical to drug discovery, guiding chemists in turning initial molecular hits into drug-like candidates. Unlike unconstrained molecule generation Gómez-Bombarelli et al. (2018); Jin et al. (2019), molecular editing involves targeted modifications, such as scaffold decoration, fragment substitutions, or precise structural refinements, that carefully balance therapeutic properties with chemical feasibility and synthetic practicality Seo et al. (2023); Jinsong et al. (2024).

To assist chemists in this iterative lead optimization process, recent approaches leverage large language models (LLMs), either through fine-tuning or by using them as reasoning agents capable of interpreting textual prompts (e.g. "increase solubility") and proposing relevant molecular edits Zimmermann et al. (2025); Mirza et al. (2025a). Additionally, reinforcement learning (RL)-based post-training can align these models even more closely with practical constraints, improving both chemical plausibility and edit precision Dai et al. (2025); Liu et al. (2025). Progress, however, is limited by data. Training and evaluating editing models requires goal-aligned edit datasets that pair a parent molecule with a proposed child and standardized outcomes, at a scale that supports both supervised fine-tuning and post-training Polykovskiy et al. (2020); Huang et al. (2021). Nevertheless, existing corpora either lack the scale required for robust training or omit explicit edit annotations needed for guided policy learning.

To close this gap, we curate MEGA (Molecular Editing with Guided Action), a large-scale, molecule editing dataset of (parent, child) molecule pairs spanning 28 tasks. The dataset is offered in in two scales, the primary MEGA dataset, containing 522 thousand successful edits, and an expanded version, MEGA-Large, with 31.4 million positive samples. We also release an additional 41 million valid and chemically close negative examples to enable contrastive learning and Reinforcement Learning (RL) reward shaping Robinson et al. (2021); Shen et al. (2024).

Using a fixed LLM and a shared evaluation protocol, we first quantify the effect of data alone by fine-tuning on MEGA versus other public datasets. We then show that post-training with GRPO Shao et al. (2024), using a composite reward that combines a thresholded property gain term and a Tanimoto similarity term Bajusz et al. (2015), yields further gains with reduced number of training samples.

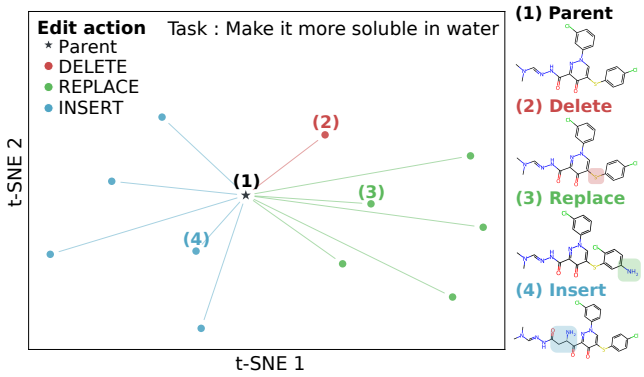

Figure 1: Morgan-fingerprint t-SNE for a parent SMILES and child molecules generated by fragment edits, delete, replace, insert. Colors encode the applied edit, highlighting neighborhood exploration under the given task.

Concretely, this work introduces the following contributions:

1. We release MEGA, a family of molecular editing datasets with fragment-level *Replace*, *Insert*, and *Delete* annotations. It contains two variants: MEGA (522K pairs) for resource-constrained regimes, and MEGA-Large (31.4M pairs) for scaling studies. MEGA-Large is over an order of magnitude larger than any existing dataset for molecular editing.
2. We demonstrate that under fixed model and training protocol, fine-tuning on MEGA increases hit ratios by up to +21.47 percentage points over established datasets on shared tasks, while its explicit edit labels enable per-action supervision and diagnostics.
3. We show that GRPO post-training on MEGA with a similarity-aware reward improves property alignment and edit minimality, while also achieving state-of-the-art performance on established benchmarks. With only 14K training examples, the GRPO post-trained model matches the performance of the SFT model trained on the full MEGA set, corresponding to a $\sim 36\times$ improvement in data efficiency.

2 Related Work

2.1 Datasets for Molecular Editing

Public corpora vary in task formulation and scale. MoleculeSTM Liu et al. (2023a) trains a multimodal structure–text model on hundreds of thousands of molecule–caption pairs through contrastive learning and proposes instruction-guided retrieval and editing tasks, establishing a text-based benchmark for property-aware modification. Another example is MolOpt-Instructions Ye et al. (2025), released alongside DrugAssist, which compiles a large instruction dataset to fine-tune language models for molecule optimization from natural language goals. Furthermore, MolEdit-Instruct Zhuang et al. (2025) scales property-conditioned edits by pairing each parent molecule with an explicit edit instruction and target property change. The dataset is used to evaluate diffusion and RL models under joint constraints on molecular similarity and property improvement, reflecting a shift toward instruction-plus-constraint benchmarks. Together, these datasets illustrate the available range for training and evaluating molecular editing models, despite differences in construction, supervision signals, and scale.

2.2 LLMs for Chemistry

General-purpose language models trained on broad text data already exhibit useful zero-shot chemistry skills answering property prediction questions, translating line notations, or suggesting functional-group swaps straight out of the box Liu et al. (2023b); Bran et al. (2025); Mirza et al.

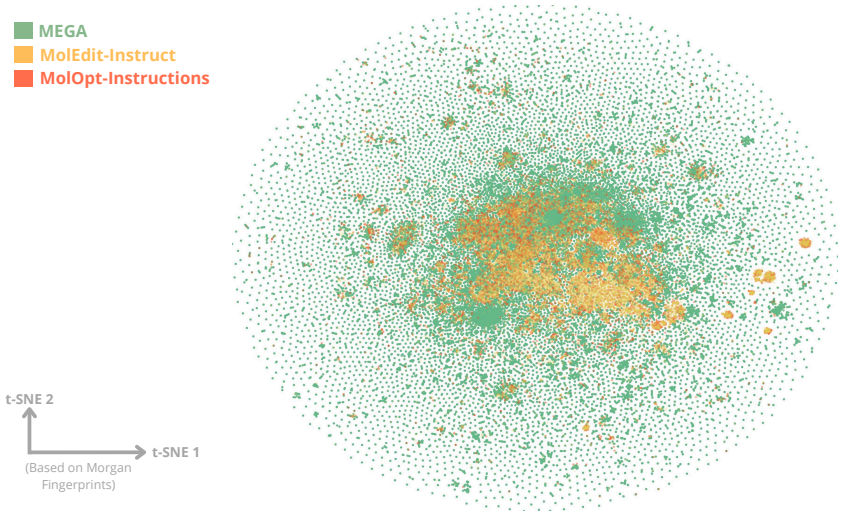

Figure 2: t-SNE projection of Morgan fingerprints showing chemical space coverage of statistical significant subsets of MEGA, MolEdit-Instruct, and MolOpt-Instructions.

(2025b). When wrapped in a tool-calling framework, the same models can act as agents: ChemCrow, for example, prompts an off-the-shelf LLM to invoke cheminformatics utilities (parsers, property predictors, similarity search) and carry out multi-step design tasks from natural language instructions M. Bran et al. (2024).

Researchers also adapt these open language models to chemistry via domain fine-tuning and task-specific supervision. For instance, LlamoLe trains on ∼128k USPTO reactions with textual descriptions to strengthen reasoning and route identification Lowe (2017); Liu et al. (2024), while DrugAssist uses MolOpt-Instructions to instruction-tune models for property-directed optimization from text in a single-shot fashion Ye et al. (2025).

A further layer of refinement uses reinforcement learning such as with Ether0, trained on 640k experimentally-grounded chemistry problems across 375 tasks, to excel at tasks like retrosynthesis and solubility editing Narayanan et al. (2025). Another example is MolEditRL, which pairs property-conditioned prompts with structure-preserving edit operators and reinforcement-style objectives to promote local, similarity-respecting modifications Zhuang et al. (2025).

2.3 Editors Beyond LLMs for Lead Optimization

While LLM-based editors are comparatively recent, lead optimization has a long history of non-LLM approaches that emphasize local, property-directed modifications to a given scaffold. Earlier rule-based strategies, such as matched molecular pairs (MMPs) Yang et al. (2023) and fixed reaction templates, encoded medicinal-chemistry heuristics for systematic substitution. More recent machine learning methods operate directly on strings or graphs to propose minimal edits, including JT-VAE Jin et al. (2019), GCPN You et al. (2019), and MARS Xie et al. (2021); Loeffler et al. (2024). In parallel, diffusion models adapt continuous generative dynamics to discrete molecular modifications: DiffLink designs linkers between fixed fragments Igashov et al. (2024), while DiffHop performs constrained scaffold hopping Torge et al. (2023). Taken together, these approaches chart a progression from rules to learned editors to diffusion frameworks, all aimed at controllable, chemically plausible edits central to lead optimization.

3 MEGA Dataset

3.1 Dataset Construction Overview

MEGA is a family of large-scale datasets with a total of 31.4M parent–child SMILES pairs. Each child comes from applying a single functional-group edit to a ZINC250K parent, without a con-

Table 1: Comparison of molecular editing datasets used in this study. Reported sizes count only successful (positive) parent-child pairs. Unique molecules counts distinct SMILES across both parents and children. Action provided indicates whether a dataset records the edit label.

Dataset	Size	Unique Molecules	# Tasks	Action Provided
MoleculeSTM	280K	250K	34	No
MolEdit-Instruct	3.03M	967K	20	No
MolOpt-Instructions	1.24M	1.596M	16	No
MEGA	522K	372K	28	Yes
MEGA-Large	31.4M	22.126M	28	Yes

straint to preserve the scaffold Irwin & Shoichet (2005). Candidate modification sites are located with established retrosynthetic slicing rules (BRICS Degen et al. (2008), Hussain–Rea (HR) Hussain & Rea (2010) and RECAP Lewell et al. (1998)) and exactly one action is applied at a chosen site: *Delete*, *Insert*, or *Replace* a functional group. The child is rebuilt and sanitized in RDKit Landrum & Contributors (2025), and task properties are computed deterministically. We adopt the MoleculeSTM protocol for task labeling: for each objective (e.g. "increase solubility"), we use RDKit to verify whether the child clears the threshold for that task. Each record includes parent SMILES, child SMILES, a coarse action tag (*Insert*/*Delete*/*Replace*), the task identifier and threshold level, and the parent/child property vectors. The computational budget for MEGA amounted to approximately 184k CPU-hours on a 128-core cluster.

For efficient training, we define MEGA as a uniformly sampled subset of 522K positive examples drawn from the full 31M-pair dataset, which we refer to as MEGA-Large. MEGA mirrors the action distribution of MEGA-Large (3.1% *Delete*, 43.6% *Insert*, 53.3% *Replace*), making it suitable for resource-constrained settings while retaining the statistical properties of the full collection. In addition to the positives, we also provide 41 million valid but chemically close negative pairs that, while not meeting the improvement threshold, offer valuable hard negatives for contrastive learning or reinforcement learning setups.

To emphasize drug discovery relevance, our tasks target widely used objectives including aqueous solubility, drug-likeness (QED), H-bond donors/acceptors, permeability proxies and topological polar surface area (TPSA). Each one evaluated at two thresholds, loose and strict. Restricting edits to a single modification per pair enables controlled exploration of the parent's local chemical neighborhood. A parent molecule may appear in multiple pairs if it contains eligible sites for several actions across tasks. For each edit–task combination, we retain up to five successful and five near-miss children, ranked to maximize diversity while avoiding redundancy. Further details on tasks and dataset composition are provided in Appendix A.

3.2 Dataset Coverage

Figure 1 shows a representative parent alongside three children, one per action. The edits are local and chemically rational: removing an atom (*Delete*), adding a small moiety (*Insert*) or swapping one group for another (*Replace*). Together they illustrate the targeted nature of MEGA's pairs. In this example, all children satisfy the "increase aqueous solubility" objective.

Figure 2 visualizes a statistically significant subset of MEGA in the 2048-bit Morgan-fingerprint space Morgan (1965) using t-SNE van der Maaten & Hinton (2008). The overlay shows that MEGA occupies the shared high-density core with existing molecular editing datasets and also reaches beyond it, consistent with its scale and edit policy. Moreover, Table 1 quantifies this comparison: in terms of successful (positive) edits, the full set is roughly an order of magnitude larger than the next largest dataset. Furthermore, unlike other datasets, MEGA includes a coarse action label (*Insert*/*Delete*/*Replace*) for every pair, supporting per-action supervision, diagnostics, and reproducibility.

Table 2: Performance comparison of SFT models on shared molecular editing tasks. The best results are marked in bold. We report the mean and std of five runs.

Task	Description	Threshold	Dataset		
			MEGA	MolEdit Instruct	MolOpt Instruction
103	*More like a drug*	0.0	**62.46 ± 2.18**	23.92 ± 0.99	16.38 ± 2.03
		0.1	**28.43 ± 1.38**	12.85 ± 0.58	8.38 ± 0.53
104	*Less like a drug*	0.0	97.81 ± 0.91	**98.97 ± 0.33**	96.87 ± 0.82
		0.1	83.94 ± 3.43	**98.86 ± 0.51**	94.43 ± 1.47
107	*More H-bond acceptors*	0.0	**99.28 ± 0.25**	94.96 ± 1.70	89.33 ± 1.18
		1.0	**93.06 ± 0.66**	43.35 ± 1.65	34.06 ± 0.58
108	*More H-bond donors*	0.0	**99.80 ± 0.25**	97.66 ± 0.59	96.21 ± 0.91
		1.0	**99.29 ± 0.25**	67.57 ± 1.78	56.67 ± 1.10
Average			**83.01**	67.27	61.54

4 EXPERIMENTS

We evaluate MEGA in a two-stage protocol: (1) supervised fine-tuning (SFT) to benchmark performance under identical model and training settings against existing datasets, and (2) RL post-training with a hybrid reward combining property gains and structural similarity. We also analyze edit action distributions, locality, and sample efficiency in single- and multi-objective tasks.

4.1 SUPERVISED FINE-TUNING

Protocol. We fine-tune a Llama-3 8B model Dubey et al. (2024) with LoRA adapters Hu et al. (2021) on MolOpt Instruction, MolEdit Instruct, and MEGA. All runs use the same hyperparameters, training schedule, and LoRA configuration. Training last approximately 23 H100-equivalent hours per model until the validation loss no longer improves.

Evaluation follows the MoleculeSTM protocol Liu et al. (2023a) and is restricted to the 4 single-objective tasks shared by all three datasets. The test set contains 200 unique parent SMILES not present in any of the training sets. For each task, we assess performance at two property thresholds (loose and strict) and report the hit ratio, defined as the fraction of generated molecules that achieve the required property improvement. Each experiment is repeated five times, with a decoding temperature of 1.0, and we report the mean and standard deviation of the hit ratio across runs. The resulting models are referred to as MEGA SFT. For further comparisons and training settings details see Appendix B.

Results. Table 2 shows that the LLM trained on MEGA outperforms the same architecture trained on MolEdit Instruct and MolOpt Instruction by +15.74 (pp) and +21.47 (pp), respectively. The largest gain occurs in the "more like a drug" objective, a target known to be particularly challenging due to its composite nature Liu et al. (2023b). Variance is low and comparable to the other benchmarks, indicating that improvements are stable across repeated evaluations.

4.2 REWARD-GUIDED POST-TRAINING

Protocol. We further refine the best checkpoint from above using GRPO Shao et al. (2024) to improve property alignment while preserving local edits. During training, for each parent SMILES, the model generates a batch of multiple candidates, which are scored relative to each other. This feedback is used for updating the model weights. The scalar reward is defined as:

$$R = \underbrace{\mathbb{1}[\Delta p(\text{parent}, \text{child}) \geq \tau]}_{\text{property hit}} + \gamma \underbrace{\mathbb{1}_{\text{valid}}(\text{child})}_{\text{validity hit}} + \lambda \underbrace{h_{\tan}(\text{parent}, \text{child})}_{\text{Tanimoto hit level}}$$

Table 3: Comparison of DrugAssist, Gemini 2.5 Pro, and MEGA-GRPO across five shared tasks from the DrugAssist benchmark, evaluated under loose and strict thresholds.

Task	Description	Threshold	Model		
			DrugAssist	Gemini 2.5 Pro	MEGA GRPO
101	*More soluble in water*	0	80.00	82.23	**97.49**
		0.5	41.00	59.45	**91.10**
103	*More like a drug*	0	76.00	60.14	**83.49**
		0.1	**63.00**	23.46	50.00
107	*More H-bond acceptors*	0	71.00	64.97	**98.60**
		1	67.00	5.57	**86.74**
108	*More H-bond donors*	0	72.00	73.54	**99.31**
		1	76.00	6.32	**91.45**
201	*More soluble & more HBA*	0 - 0	50.00	80.32	**95.19**
		0.5 - 1	27.00	24.43	**84.21**
Average			62.30	48.05	**87.76**

$$h_{\tan}(\text{parent}, \text{child}) = \begin{cases} 1.0, & \text{if } T > 0.65, \\ 0.5, & \text{if } 0.4 \leq T \leq 0.65, \\ 0.0, & \text{otherwise}, \end{cases}$$

where the first term awards a hit when the property change Δp meets or exceeds the task threshold τ, the second term rewards valid and sanitized child smiles, and the third rewards scaffold-local modifications via Tanimoto coefficient discretization. The coefficients γ and λ were selected empirically to 1.0. We train with 3,000 rollouts per task under a KL-constrained objective. To assess the data efficiency of the post-training stage, we repeat this experiment with training sets ranging from 1.4k parent SMILES up to the full MEGA dataset. The resulting models are referred to as MEGA GRPO. Complete experimental details are provided in Appendix C.

We first compare MEGA GRPO against DrugAssist Zhuang et al. (2025), a state-of-the-art specialized LLM, and Gemini 2.5 Pro Comanici et al. (2025), a strong general-purpose LLM, on five single- and multi-objective molecular editing tasks. For this evaluation, we use the 500-SMILES test set provided by DrugAssist and report hit ratios under both loose and strict thresholds in Table 3.

We then compare MEGA GRPO against ChatDrug Turbo, a strong in-context learning LLM, and MoleculeSTM, a contrastive-trained encoder–decoder, on the full 28-task suite of the MEGA dataset. For this evaluation, we follow the same protocol described in the SFT section and report results in Table 4. We verified that none of the test SMILES appeared in our training data to maintain evaluation integrity.

Results. MEGA GRPO outperforms both DrugAssist and Gemini 2.5 Pro on the DrugAssist benchmark (Table 3), achieving the highest hit ratio in 9 of 10 settings. The most pronounced gains appear on the dual-objective solubility + HBA task (201), where it reaches 95.19% under loose and 84.21% under strict thresholds, substantially ahead of both baselines. The only case where MEGA GRPO underperforms is the strict drug-likeness objective, where DrugAssist retains an edge. Gemini 2.5 Pro consistently trails, particularly under strict thresholds, underscoring the difficulty of zero-shot general-purpose LLMs in molecular editing.

On the 28-task MoleculeSTM benchmark (Table 4), MEGA GRPO attains the best mean hit ratio on all task/threshold pairs. It reaches $\geq$95% on most single-property edits under loose thresholds (e.g., 101–102, 104, 106–108) and remains strong under stricter criteria. The notable hard case is Task 103 (drug-likeness), where absolute rates drop for all methods; even so, MEGA GRPO leads by 14 pp (62.60 vs. 48.65) at loose and 7 pp (26.75 vs. 19.37) at strict. MEGA GRPO's advantage is most pronounced on multi-objective tasks (201, 203, and 206), indicating better balancing of potentially competing constraints. Variance across runs is small (typically $\leq$ 1.5), suggesting the gains are stable across several runs. Overall, MEGA GRPO establishes a robust state-of-the-art

Table 4: Performance comparison of MEGA GRPO against editing methods across single and multi objective tasks and thresholds. We report the mean and standard deviation over five runs. The best results are shown in bold.

Task	Threshold	Random	MoleculeSTM	ChatDrug Turbo	MEGA GRPO
101	0	35.33±1.31	61.87±2.67	94.13±1.04	**99.31±0.10**
	0.5	11.04±2.40	49.02±1.84	88.67±0.95	**94.43±0.24**
102	0	43.36±3.06	52.71±1.67	96.86±1.10	**99.71±0.21**
	0.5	19.75±1.56	30.47±3.26	70.08±3.44	**95.52±0.51**
103	0	38.06±2.57	36.52±2.46	48.65±3.39	**62.60±2.41**
	0.1	5.27±0.24	8.81±0.82	19.37±5.54	**26.75±1.64**
104	0	36.96±2.25	58.59±1.01	70.75±2.92	**97.55±0.64**
	0.1	6.16±1.87	37.56±1.76	30.99±2.66	**93.63±0.56**
105	0	25.23±2.13	57.74±0.60	56.56±1.84	**90.19±1.34**
	10	17.41±1.43	47.51±1.88	43.08±2.95	**87.88±0.94**
106	0	16.79±2.54	34.13±0.59	77.35±1.98	**100.00±0.00**
	10	11.02±0.71	26.48±0.97	66.69±2.74	**99.43±0.01**
107	0	12.64±1.64	54.01±5.26	95.35±0.62	**99.86±0.29**
	1	0.69±0.01	27.33±2.62	72.60±2.51	**92.35±0.50**
108	0	2.97±0.61	28.55±0.76	96.54±1.31	**98.45±0.83**
	1	0.00±0.00	7.69±0.56	76.43±3.32	**95.22±0.34**
201	0 – 0	9.88±1.03	27.87±3.86	79.62±0.64	**98.53±0.44**
	0.5 – 1	0.23±0.33	8.80±0.04	49.64±2.66	**90.34±0.47**
202	0 – 0	2.99±0.38	8.55±2.75	51.59±3.79	**97.24±0.92**
	0.5 – 1	0.45±0.32	2.93±0.30	24.92±4.85	**92.04±0.53**
203	0 – 0	2.28±1.15	33.51±4.08	89.34±0.96	**99.64±0.48**
	0.5 – 1	0.00±0.00	9.98±1.03	53.64±5.81	**98.35±0.90**
204	0 – 0	0.69±0.58	17.03±2.75	39.90±3.86	**92.60±1.44**
	0.5 – 1	0.00±0.00	2.59±1.14	24.19±2.19	**60.06±1.83**
205	0 – 0	5.06±1.21	35.69±3.19	12.85±2.68	**89.30±0.93**
	0.5 – 10	1.16±0.68	19.15±0.73	10.44±5.75	**82.86±0.75**
206	0 – 0	12.17±1.05	44.35±0.68	65.33±2.16	**99.54±0.43**
	0.5 – 10	6.20±0.64	28.67±2.22	52.90±2.23	**94.31±0.23**

baseline for both single- and multi-objective molecular editing. These outcomes reflect the synergy between the MEGA dataset and locality-aware GRPO training. MEGA provides informative and diverse demonstrations of guided optimization through single-local edits, while GRPO with Tanimoto similarity further aligns the model's behavior with task-specific reward signals. For further details, see Appendix D.

Data Efficiency. Figure 3 shows that GRPO with Tanimoto reward outperforms SFT across all data regimes while maintaining scaffold edits within our targeted Tanimoto similarity range (0.6–0.8). With only 14k training examples, MEGA GRPO (14K) matches the performance of MEGA SFT trained on 522k by +2.11 pp, achieving $\sim 36\times$ data efficiency multiplier with the same Llama 3 base model.

Guided-Action Editing. Figure 4 shows the distribution of fragment-level edit actions across tasks. The MEGA SFT model roughly reproduce the action distribution of the MEGA dataset. This indicates internalization of single-fragment edit patterns (replace, insert, delete) present in the demonstrations. In contrast, MEGA GRPO learns, via RL, heavily favors *replace* actions, reflecting an optimization bias towards minimal yet property-aligned functional group modifications. The

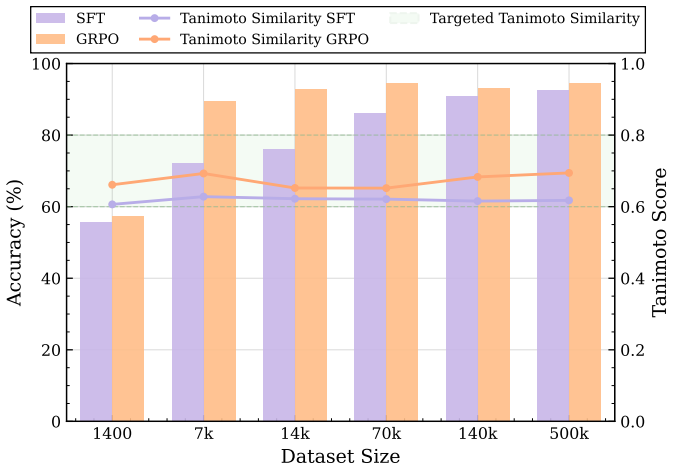

Figure 3: Data efficiency comparison of SFT and GRPO across training set sizes (based on loose threshold). GRPO consistently outperforms SFT while keeping edits within the targeted Tanimoto similarity range (0.6–0.8).

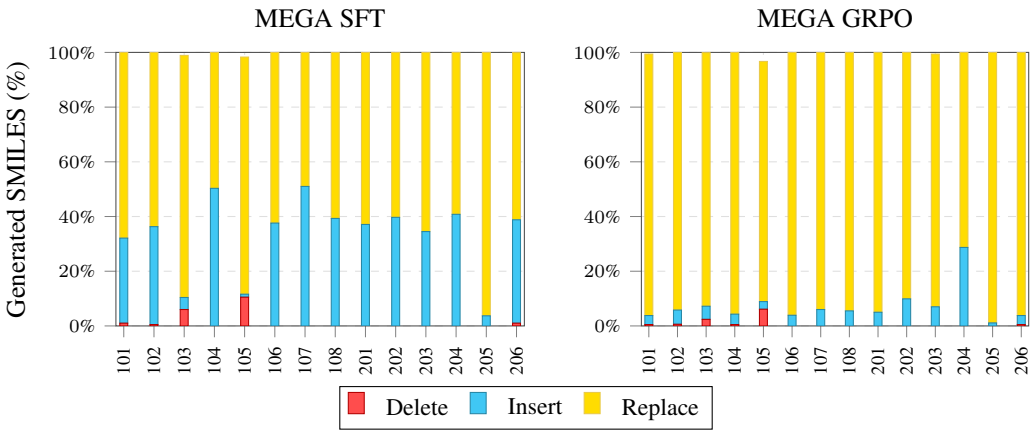

Figure 4: Distribution of fragment-level edit actions during inference for MEGA SFT (522K) and MEGA GRPO (14K), on single and double-molecule optimization tasks.

performance increase of the GRPO model, suggest that replace-dominant strategies are, on average, more efficient than the dataset's action distribution.

5 Conclusion

In this work, we release MEGA, a family of large-scale datasets comprising 31.4M molecule pairs designed to advance property-guided molecular editing. By systematically generating single chemically rational edits that improve a target property (*replace*, *insert*, *delete*), MEGA provides dense, high-quality supervision for exploring local chemical space. Our experiments demonstrate its value: models fine-tuned on MEGA significantly outperform those trained on existing datasets in supervised settings. Furthermore, when combined with RL post-training, models trained on MEGA achieve state-of-the-art performance on established benchmarks and demonstrate a remarkable $\sim 36\times$ improvement in data efficiency. By providing controlled, high-quality examples at scale, MEGA enables the development of stronger generative models and more effective molecular optimization workflows.

6 Reproducibility Statement

The construction of the dataset is described in Section 3.1, with additional licensing details provided in Appendix F. The dataset is released under the same license as the source dataset from which it is derived. Scripts for training and evaluation, including both finetuning and post-training procedures, will be made available in a public repository under a permissive license. These resources, along with the detailed experimental settings reported in the main text and appendix, are intended to ensure full reproducibility of our results and maximize benefit to the research community.

7 Ethical Statement

The authors have considered the ethical implications of this work and find no direct ethical concerns. All research was performed on publicly available datasets and did not involve human subjects or personally identifiable information. The authors also declare no conflicts of interest.

8 Use of Large Language Models

Large Language Models (LLMs) were used in a limited capacity as a writing and coding assistant. Specifically, LLMs were used to:

- Improve clarity, grammar, and flow in parts of the manuscript.
- Suggest structure for some sections of text.
- Assist with debugging of boilerplate code, without contributing novel algorithmic ideas.

All substantive research ideas, experimental design, analysis, and conclusions were developed entirely by the authors. The authors take full responsibility for the accuracy and integrity of all content presented.

References

Tagir Akhmetshin, Arkadii I. Lin, Daniyar Mazitov, Evgenii Ziaikin, Timur Madzhidov, and Alexandre Varnek. ZINC 250K data sets. 12 2021. doi: 10.6084/m9.figshare.17122427.v1. URL https://figshare.com/articles/dataset/ZINC_250K_data_sets/17122427.

Dávid Bajusz, Anita Rácz, and Károly Héberger. Why is tanimoto index an appropriate choice for fingerprint-based similarity calculations? *Journal of cheminformatics*, 7(1):20, 2015.

Andres M Bran, Theo A Neukomm, Daniel P Armstrong, Zlatko Jončev, and Philippe Schwaller. Chemical reasoning in llms unlocks strategy-aware synthesis planning and reaction mechanism elucidation, 2025. URL https://arxiv.org/abs/2503.08537.

Gheorghe Comanici, Eric Bieber, Mike Schaekermann, Ice Pasupat, Noveen Sachdeva, Inderjit Dhillon, Marcel Blistein, Ori Ram, Dan Zhang, Evan Rosen, et al. Gemini 2.5: Pushing the frontier with advanced reasoning, multimodality, long context, and next generation agentic capabilities. *arXiv preprint arXiv:2507.06261*, 2025.

Weichen Dai, Zijie Dai, Zhijie Huang, Yixuan Pan, Xinhe Li, Xi Li, Yi Zhou, Ji Qi, and Wu Jiang. Rldbf: Enhancing llms via reinforcement learning with database feedback, 2025. URL https://arxiv.org/abs/2504.03713.

Jörg Degen, Christof Wegscheid-Gerlach, Andrea Zaliani, and Matthias Rarey. On the art of compiling and using 'drug-like' chemical fragment spaces. *ChemMedChem*, 3(10):1503–1507, October 2008.

Abhimanyu Dubey, Abhinav Jauhri, Abhinav Pandey, Abhishek Kadian, Ahmad Al-Dahle, Aiesha Letman, Akhil Mathur, Alan Schelten, Amy Yang, Angela Fan, et al. The llama 3 herd of models. *arXiv e-prints*, pp. arXiv–2407, 2024.

Rafael Gómez-Bombarelli, Jennifer N. Wei, David Duvenaud, José Miguel Hernández-Lobato, Benjamín Sánchez-Lengeling, Dennis Sheberla, Jorge Aguilera-Iparraguirre, Timothy D. Hirzel, Ryan P. Adams, and Alán Aspuru-Guzik. Automatic chemical design using a data-driven continuous representation of molecules. *ACS Central Science*, 4(2):268–276, 2018. doi: 10.1021/acscentsci.7b00572. URL https://doi.org/10.1021/acscentsci.7b00572. PMID: 29532027.

Edward J. Hu, Yelong Shen, Phillip Wallis, Zeyuan Allen-Zhu, Yuanzhi Li, Shean Wang, Lu Wang, and Weizhu Chen. Lora: Low-rank adaptation of large language models, 2021. URL https://arxiv.org/abs/2106.09685.

Kexin Huang, Tianfan Fu, Wenhao Gao, Yue Zhao, Yusuf Roohani, Jure Leskovec, Connor W. Coley, Cao Xiao, Jimeng Sun, and Marinka Zitnik. Therapeutics data commons: Machine learning datasets and tasks for drug discovery and development, 2021. URL https://arxiv.org/abs/2102.09548.

Jameed Hussain and Ceara Rea. Computationally efficient algorithm to identify matched molecular pairs (mmps) in large data sets. *Journal of Chemical Information and Modeling*, 50(3):339–348, 2010. doi: 10.1021/ci900450m. URL https://doi.org/10.1021/ci900450m. PMID: 20121045.

Ilia Igashov, Hannes Stärk, Clément Vignac, Arne Schneuing, Victor Garcia Satorras, Pascal Frossard, Max Welling, Michael Bronstein, and Bruno Correia. Equivariant 3d-conditional diffusion model for molecular linker design. *Nature Machine Intelligence*, 6(4):417–427, April 2024.

John J Irwin and Brian K Shoichet. ZINC–a free database of commercially available compounds for virtual screening. *J Chem Inf Model*, 45(1):177–182, January 2005.

Wengong Jin, Regina Barzilay, and Tommi Jaakkola. Junction tree variational autoencoder for molecular graph generation, 2019. URL https://arxiv.org/abs/1802.04364.

Shao Jinsong, Jia Qifeng, Chen Xing, Yajie Hao, and Li Wang. Molecular fragmentation as a crucial step in the AI-based drug development pathway. *Communications Chemistry*, 7(1):20, February 2024.

Greg Landrum and RDKit Contributors. RDKit: Open-source cheminformatics, 2025. URL https://doi.org/10.5281/zenodo.591637. This concept DOI covers all RDKit versions on Zenodo and always resolves to the latest release.

X Q Lewell, D B Judd, S P Watson, and M M Hann. RECAP–retrosynthetic combinatorial analysis procedure: a powerful new technique for identifying privileged molecular fragments with useful applications in combinatorial chemistry. *J Chem Inf Comput Sci*, 38(3):511–522, May 1998.

Gang Liu, Michael Sun, Wojciech Matusik, Meng Jiang, and Jie Chen. Multimodal large language models for inverse molecular design with retrosynthetic planning, 2024. URL https://arxiv.org/abs/2410.04223.

Shengchao Liu, Weili Nie, Chengpeng Wang, Jiarui Lu, Zhuoran Qiao, Ling Liu, Jian Tang, Chaowei Xiao, and Anima Anandkumar. Multi-modal molecule structure-text model for text-based retrieval and editing. *Nature Machine Intelligence*, 5(12):1447–1457, 2023a.

Shengchao Liu, Jiongxiao Wang, Yijin Yang, Chengpeng Wang, Ling Liu, Hongyu Guo, and Chaowei Xiao. Chatgpt-powered conversational drug editing using retrieval and domain feedback, 2023b. URL https://arxiv.org/abs/2305.18090.

Xuefeng Liu, Songhao Jiang, Siyu Chen, Zhuoran Yang, Yuxin Chen, Ian Foster, and Rick Stevens. Drugimprovergpt: A large language model for drug optimization with fine-tuning via structured policy optimization, 2025. URL https://arxiv.org/abs/2502.07237.

Hannes H Loeffler, Jiazhen He, Alessandro Tibo, Jon Paul Janet, Alexey Voronov, Lewis H Mervin, and Ola Engkvist. Reinvent 4: Modern AI–driven generative molecule design. *Journal of Cheminformatics*, 16(1):20, February 2024.

Daniel Lowe. Chemical reactions from US patents (1976-Sep2016). 6 2017. doi: 10.6084/m9.figshare.5104873.v1. URL https://figshare.com/articles/dataset/Chemical_reactions_from_US_patents_1976-Sep2016_/5104873.

Andres M. Bran, Sam Cox, Oliver Schilter, Carlo Baldassari, Andrew D White, and Philippe Schwaller. Augmenting large language models with chemistry tools. *Nature Machine Intelligence*, 6(5):525–535, May 2024.

Adrian Mirza, Nawaf Alampara, Sreekanth Kunchapu, Martiño Ríos-García, Benedict Emoekabu, Aswanth Krishnan, Tanya Gupta, Mara Schilling-Wilhelmi, Macjonathan Okereke, Anagha Aneesh, Mehrdad Asgari, Juliane Eberhardt, Amir Mohammad Elahi, Hani M Elbeheiry, María Victoria Gil, Christina Glaubitz, Maximilian Greiner, Caroline T Holick, Tim Hoffmann, Abdelrahman Ibrahim, Lea C Klepsch, Yannik Köster, Fabian Alexander Kreth, Jakob Meyer, Santiago Miret, Jan Matthias Peschel, Michael Ringleb, Nicole C Roesner, Johanna Schreiber, Ulrich S Schubert, Leanne M Stafast, A D Dinga Wonanke, Michael Pieler, Philippe Schwaller, and Kevin Maik Jablonka. A framework for evaluating the chemical knowledge and reasoning abilities of large language models against the expertise of chemists. *Nature Chemistry*, 17(7): 1027–1034, July 2025a.

Adrian Mirza, Nawaf Alampara, Sreekanth Kunchapu, Martiño Ríos-García, Benedict Emoekabu, Aswanth Krishnan, Tanya Gupta, Mara Schilling-Wilhelmi, Macjonathan Okereke, Anagha Aneesh, Mehrdad Asgari, Juliane Eberhardt, Amir Mohammad Elahi, Hani M Elbeheiry, María Victoria Gil, Christina Glaubitz, Maximilian Greiner, Caroline T Holick, Tim Hoffmann, Abdelrahman Ibrahim, Lea C Klepsch, Yannik Köster, Fabian Alexander Kreth, Jakob Meyer, Santiago Miret, Jan Matthias Peschel, Michael Ringleb, Nicole C Roesner, Johanna Schreiber, Ulrich S Schubert, Leanne M Stafast, A D Dinga Wonanke, Michael Pieler, Philippe Schwaller, and Kevin Maik Jablonka. A framework for evaluating the chemical knowledge and reasoning abilities of large language models against the expertise of chemists. *Nature Chemistry*, 17(7): 1027–1034, July 2025b.

H. L. Morgan. The generation of a unique machine description for chemical structures-a technique developed at chemical abstracts service. *Journal of Chemical Documentation*, 5(2):107–113, 1965. doi: 10.1021/c160017a018. URL https://doi.org/10.1021/c160017a018.

Siddharth M. Narayanan, James D. Braza, Ryan-Rhys Griffiths, Albert Bou, Geemi Wellawatte, Mayk Caldas Ramos, Ludovico Mitchener, Samuel G. Rodriques, and Andrew D. White. Training a scientific reasoning model for chemistry, 2025. URL https://arxiv.org/abs/2506.17238.

Daniil Polykovskiy, Alexander Zhebrak, Benjamin Sanchez-Lengeling, Sergey Golovanov, Oktai Tatanov, Stanislav Belyaev, Rauf Kurbanov, Aleksey Artamonov, Vladimir Aladinskiy, Mark Veselov, Artur Kadurin, Simon Johansson, Hongming Chen, Sergey Nikolenko, Alán Aspuru-Guzik, and Alex Zhavoronkov. Molecular sets (MOSES): A benchmarking platform for molecular generation models. *Front Pharmacol*, 11:565644, December 2020.

Kristina Preuer, Philipp Renz, Thomas Unterthiner, Sepp Hochreiter, and Gunter Klambauer. Fréchet chemnet distance: a metric for generative models for molecules in drug discovery. *Journal of chemical information and modeling*, 58(9):1736–1741, 2018.

Joshua Robinson, Ching-Yao Chuang, Suvrit Sra, and Stefanie Jegelka. Contrastive learning with hard negative samples, 2021. URL https://arxiv.org/abs/2010.04592.

Seonghwan Seo, Jaechang Lim, and Woo Youn Kim. Molecular generative model via retrosynthetically prepared chemical building block assembly. *Adv Sci (Weinh)*, 10(8):e2206674, January 2023.

Zhihong Shao, Peiyi Wang, Qihao Zhu, Runxin Xu, Junxiao Song, Xiao Bi, Haowei Zhang, Mingchuan Zhang, Y. K. Li, Y. Wu, and Daya Guo. Deepseekmath: Pushing the limits of mathematical reasoning in open language models, 2024. URL https://arxiv.org/abs/2402.03300.

Wei Shen, Xiaoying Zhang, Yuanshun Yao, Rui Zheng, Hongyi Guo, and Yang Liu. Improving reinforcement learning from human feedback using contrastive rewards, 2024. URL https://arxiv.org/abs/2403.07708.

Jos Torge, Charles Harris, Simon V. Mathis, and Pietro Lio. Diffhopp: A graph diffusion model for novel drug design via scaffold hopping, 2023. URL https://arxiv.org/abs/2308.07416.

Laurens van der Maaten and Geoffrey Hinton. Visualizing data using t-sne. *Journal of Machine Learning Research*, 9(86):2579–2605, 2008. URL http://jmlr.org/papers/v9/vandermaaten08a.html.

Yutong Xie, Chence Shi, Hao Zhou, Yuwei Yang, Weinan Zhang, Yong Yu, and Lei Li. Mars: Markov molecular sampling for multi-objective drug discovery, 2021. URL https://arxiv.org/abs/2103.10432.

Ziyi Yang, Shaohua Shi, Li Fu, Aiping Lu, Tingjun Hou, and Dongsheng Cao. Matched molecular pair analysis in drug discovery: methods and recent applications. *Journal of Medicinal Chemistry*, 66(7):4361–4377, 2023.

Geyan Ye, Xibao Cai, Houtim Lai, Xing Wang, Junhong Huang, Longyue Wang, Wei Liu, and Xiangxiang Zeng. Drugassist: a large language model for molecule optimization. *Briefings in Bioinformatics*, 26(1):bbae693, 01 2025. ISSN 1477-4054. doi: 10.1093/bib/bbae693. URL https://doi.org/10.1093/bib/bbae693.

Jiaxuan You, Bowen Liu, Rex Ying, Vijay Pande, and Jure Leskovec. Graph convolutional policy network for goal-directed molecular graph generation, 2019. URL https://arxiv.org/abs/1806.02473.

Yuanxin Zhuang, Dazhong Shen, and Ying Sun. Moleditrl: Structure-preserving molecular editing via discrete diffusion and reinforcement learning, 2025. URL https://arxiv.org/abs/2505.20131.

Yoel Zimmermann, Adib Bazgir, Zartashia Afzal, Fariha Agbere, Qianxiang Ai, Nawaf Alampara, Alexander Al-Feghali, Mehrad Ansari, Dmytro Antypov, Amro Aswad, Jiaru Bai, Viktoriia Baibakova, Devi Dutta Biswajeet, Erik Bitzek, Joshua D. Bocarsly, Anna Borisova, Andres M Bran, L. Catherine Brinson, Marcel Moran Calderon, Alessandro Canalicchio, Victor Chen, Yuan Chiang, Defne Circi, Benjamin Charmes, Vikrant Chaudhary, Zizhang Chen, Min-Hsueh Chiu, Judith Clymo, Kedar Dabhadkar, Nathan Daelman, Archit Datar, Wibe A. de Jong, Matthew L. Evans, Maryam Ghazizade Fard, Giuseppe Fisicaro, Abhijeet Sadashiv Gangan, Janine George, Jose D. Cojal Gonzalez, Michael Götte, Ankur K. Gupta, Hassan Harb, Pengyu Hong, Abdelrahman Ibrahim, Ahmed Ilyas, Alishba Imran, Kevin Ishimwe, Ramsey Issa, Kevin Maik Jablonka, Colin Jones, Tyler R. Josephson, Greg Juhasz, Sarthak Kapoor, Rongda Kang, Ghazal Khalighinejad, Sartaaj Khan, Sascha Klawohn, Suneel Kuman, Alvin Noe Ladines, Sarom Leang, Magdalena Lederbauer, Sheng-Lun, Liao, Hao Liu, Xuefeng Liu, Stanley Lo, Sandeep Madireddy, Piyush Ranjan Maharana, Shagun Maheshwari, Soroush Mahjoubi, José A. Márquez, Rob Mills, Trupti Mohanty, Bernadette Mohr, Seyed Mohamad Moosavi, Alexander Moßhammer, Amirhossein D. Naghdi, Aakash Naik, Oleksandr Narykov, Hampus Näsström, Xuan Vu Nguyen, Xinyi Ni, Dana O'Connor, Teslim Olayiwola, Federico Ottomano, Aleyna Beste Ozhan, Sebastian Pagel, Chiku Parida, Jaehee Park, Vraj Patel, Elena Patyukova, Martin Hoffmann Petersen, Luis Pinto, José M. Pizarro, Dieter Plessers, Tapashree Pradhan, Utkarsh Pratiush, Charishma Puli, Andrew Qin, Mahyar Rajabi, Francesco Ricci, Elliot Risch, Martiño Ríos-García, Aritra Roy, Tehseen Rug, Hasan M Sayeed, Markus Scheidgen, Mara Schilling-Wilhelmi, Marcel Schloz, Fabian Schöppach, Julia Schumann, Philippe Schwaller, Marcus Schwarting, Samiha Sharlin, Kevin Shen, Jiale Shi, Pradip Si, Jennifer D'Souza, Taylor Sparks, Suraj Sudhakar, Leopold Talirz, Dandan Tang, Olga Taran, Carla Terboven, Mark Tropin, Anastasiia Tsymbal, Katharina Ueltzen, Pablo Andres Unzueta, Archit Vasan, Tirtha Vinchurkar, Trung Vo, Gabriel Vogel, Christoph Völker, Jan Weinreich, Faradawn Yang, Mohd Zaki, Chi Zhang, Sylvester Zhang, Weijie Zhang, Ruijie Zhu, Shang Zhu, Jan Janssen, Calvin Li, Ian Foster, and Ben Blaiszik. Reflections from the 2024 large language model (llm) hackathon for applications in materials science and chemistry, 2025. URL https://arxiv.org/abs/2411.15221.

A MEGA DATASET DETAILS

Tasks. For curating MEGA we used single-objective tasks (101–108) that targets one property, and multi-objective tasks (201–206) for two properties. Table 5 lists the desired direction of change (↑ increase, ↓ decrease), variable name (consistent with RDKit), alongside the requirement in natural-language. For each task we evaluate 2 threshold with different levels of property change. Table 6 gives the evaluation thresholds under *loose* and *strict* criteria. For multi-objective tasks, each threshold vector follows the property order in the *Target(s)* column.

Task ID	Target(s)	Task Requirement 1	Task Requirement 2
101	$\downarrow \log P$	more soluble in water	None
102	$\uparrow \log P$	less soluble in water	None
103	$\uparrow$ QED	more like a drug	None
104	$\downarrow$ QED	less like a drug	None
105	$\downarrow$ TPSA	higher permeability	None
106	$\uparrow$ TPSA	lower permeability	None
107	$\uparrow$ HBA	more hydrogen bond acceptors	None
108	$\uparrow$ HBD	more hydrogen bond donors	None
201	$\downarrow \log P, \uparrow$ HBA	more soluble in water	more hydrogen bond acceptors
202	$\uparrow \log P, \uparrow$ HBA	less soluble in water	more hydrogen bond acceptors
203	$\downarrow \log P, \uparrow$ HBD	more soluble in water	more hydrogen bond donors
204	$\uparrow \log P, \uparrow$ HBD	less soluble in water	more hydrogen bond donors
205	$\downarrow \log P, \downarrow$ TPSA	more soluble in water	higher permeability
206	$\downarrow \log P, \uparrow$ TPSA	more soluble in water	lower permeability

Table 5: Task catalog for small-molecule property edits. All tasks require the output molecule to remain similar to the input. Arrows indicate desired property direction.

Task ID	Loose	Strict
101	`[0]`	`[0.5]`
102	`[0]`	`[0.5]`
103	`[0]`	`[0.1]`
104	`[0]`	`[0.1]`
105	`[0]`	`[10]`
106	`[0]`	`[10]`
107	`[0]`	`[1]`
108	`[0]`	`[1]`
201	`[0, 0]`	`[0.5, 1]`
202	`[0, 0]`	`[0.5, 1]`
203	`[0, 0]`	`[0.5, 1]`
204	`[0, 0]`	`[0.5, 1]`
205	`[0, 0]`	`[0.5, 10]`
206	`[0, 0]`	`[0.5, 10]`

Table 6: Evaluation thresholds per task. For multi-objective tasks, each vector's order follows the *Target(s)* order in Table 5.

Dataset Statistics. This subsection summarizes the scale and composition of MEGA-Large (31M) and MEGA (522K) and quantifies how representative the smaller split is of the full corpus. Table 7 reports dataset-level counts. MEGA-31M contains 246,532 unique parent molecules directly taken from the Zinc-250 dataset. In includes 72,366,584 evaluated edits, of which 31,354,522 are successful. MEGA mirrors this profile at smaller scale with 4,105 unique parents and 1,205,430 edits, including 522,058.

Metric	MEGA-Large (31M)	MEGA (522K)
Unique parent molecules	246,532	4,105
Successful edits	31,354,522	522,058
Unique successful SMILES	21,879,431	367,954
Negative edits	41,012,062	683,372
Unique negative SMILES	8,129,138	137,012
Total SMILES	72,366,584	1,205,430

Table 7: Side-by-side summary of MEGA datasets.

Table 8 compares the distribution of successful edits by operation. The proportions are stable across scales: `delete` ≈3.1%, `insert` ≈43.6%, and `replace` ≈53.3% in both MEGA (522K) and MEGA-Large (31M). This alignment suggests that MEGA preserves the operational mix of the full dataset and is suitable for compute-friendly budgets.

	MEGA (522K)		MEGA-Large (31M)	
Operation	**Count**	**%**	**Count**	**%**
Delete	15,924	3.1%	960,992	3.1%
Insert	227,789	43.6%	13,677,420	43.6%
Replace	278,345	53.3%	16,716,110	53.3%
Total	522,058	100%	31,354,522	100%

Table 8: Distribution of successful edit operations for MEGA-Large and MEGA.

Table 9 reports successful edits per task for MEGA-Large (31M) and MEGA (522K). Counts are broadly balanced across tasks and per-task ranking is consistent across scales. Tasks 101/102/104 yield the largest winner pools, while 103 (increase QED) and 205 (reduce $\log P$& decrease TPSA) show markedly consistent with results from the literature. MEGA preserves the relative task difficulty profile of the full corpus.

Task	MEGA-Large	MEGA
101	2,613,794	43,463
102	2,609,126	43,443
103	1,061,168	17,774
104	2,570,496	42,793
105	1,645,706	27,401
106	2,462,800	41,005
107	2,462,791	41,005
108	2,462,781	41,005
201	2,462,711	41,005
202	2,457,965	40,933
203	2,462,768	41,005
204	2,400,936	39,978
205	1,218,686	20,243
206	2,462,794	41,005
Total	**31,354,522**	**522,058**

Table 9: Number of successful edit examples per task for MEGA-Large (31M) and MEGA (522K).

Mean shifts, Table 10, align with the instructions for every task. Examples: *LogP*↓ (101) moves the mean by -0.975 (winners vs. parents) and separates winners from losers by -1.577; *LogP*↑ (102) shifts by $+0.965$ with a winner–loser gap of $+1.133$; *QED*↓ (104) shifts by -0.217; *TPSA*↑ (106) exhibits a large increase of $+31.611$; *HBA*↑ (107) and *HBD*↑ (108) increase by $+2.749$ and $+2.316$, respectively. The consistent sign and sizable winner–loser separations (last column) provide evidence of strong task-wise consistency on MEGA.

Task	Property	Obj.	Parent $\bar{x}$	Winner $\bar{x}$	Δ W–P	Loser $\bar{x}$	Δ W–L
101	LogP	↓	2.475	1.501	−0.975	3.078	−1.577
102	LogP	↑	2.475	3.440	+0.965	2.307	+1.133
103	QED	↑	0.733	0.797	+0.064	0.614	+0.183
104	QED	↓	0.733	0.516	−0.217	0.727	−0.211
105	TPSA	↓	64.918	49.669	−15.249	77.022	−27.353
106	TPSA	↑	64.918	96.530	+31.611	61.857	+34.673
107	HBA	↑	3.990	6.739	+2.749	4.224	+2.515
108	HBD	↑	1.237	3.553	+2.316	1.248	+2.305

Table 10: MEGA: mean target-property values and deltas. $\Delta_{\text{W–P}} = \bar{x}_{\text{W}} - \bar{x}_{\text{P}}$ (winners minus parents) and $\Delta_{\text{W–L}} = \bar{x}_{\text{W}} - \bar{x}_{\text{L}}$ (winners minus losers). "Winners" and "losers" correspond to successful and unsuccessful edits, on strict threshold respectively. Signs follow the task objective (increase/decrease).

Figure 5 visualizes the single-objective shifts via kernel density estimates of the target property for parent (orange) and edited child (blue) molecules. Across all eight tasks, the child distribution moves in the instructed direction (reduce/increase or count increase), demonstrating strong task-wise consistency in MEGA.

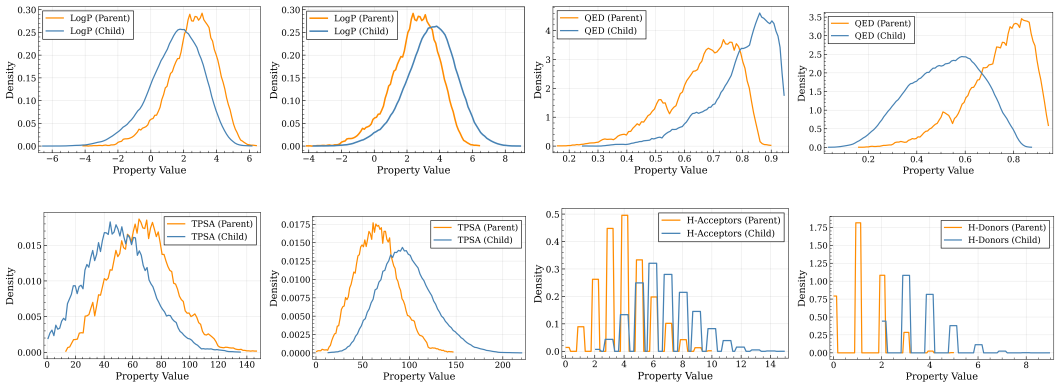

Figure 5: Molecular property distributions between parent and child molecules for MEGA.

For comparison to prior datasets, we report the Fréchet ChemNet Distance (FCD; lower is closer) (Preuer et al., 2018). As shown in Table 11, the distance between MolEdit and MolOpt roughly 4x lower compared to MEGA. This indicates that MEGA occupies a distinct region of the chemical space, while the incumbent datasets exhibit notable overlap, thus, expanding the resources available in the existing literature.

Table 11: Fréchet distance between datasets computed in Morgan-fingerprint space (lower is closer).

Dataset	MEGA	MolEdit	MolOpt
MEGA	0.000	2.790	2.738
MolEdit	2.790	0.000	0.696
MolOpt	2.738	0.696	0.000

Prompts. Unless otherwise stated, prompts request one candidate molecule in SMILES, with no extra explanation.

SINGLE-OBJECTIVE PROMPTS:

Prompt 101: Reduce $\log P$

User: Can you make molecule `SMILES`more soluble in water? The output molecule should be similar to the input molecule.
Output: One valid SMILES.

Prompt 102: Increase $\log P$

User: Can you make molecule `SMILES`less soluble in water? The output molecule should be similar to the input molecule.
Output: One valid SMILES.

Prompt 103: Increase QED

User: Can you make molecule `SMILES`more like a drug? The output molecule should be similar to the input molecule.
Output: One valid SMILES.

Prompt 104: Reduce QED

User: Can you make molecule `SMILES`less like a drug? The output molecule should be similar to the input molecule.
Output: One valid SMILES.

Prompt 105: Decrease TPSA

User: Can you make molecule `SMILES`higher permeability? The output molecule should be similar to the input molecule.
Output: One valid SMILES.

Prompt 106: Increase TPSA

User: Can you make molecule `SMILES`lower permeability? The output molecule should be similar to the input molecule.
Output: One valid SMILES.

Prompt 107: Increase HBA

User: Can you make molecule `SMILES`with more hydrogen bond acceptors? The output molecule should be similar to the input molecule.
Output: One valid SMILES.

Prompt 108: Increase HBD

User: Can you make molecule `SMILES`with more hydrogen bond donors? The output molecule should be similar to the input molecule.

Output: One valid SMILES.

TWO-OBJECTIVE PROMPTS:

Prompt 201: Reduce $\log P$ & Increase HBA

User: Can you make molecule `SMILES`more soluble in water and more hydrogen bond acceptors? The output molecule should be similar to the input molecule.
Output: One valid SMILES.

Prompt 202: Increase $\log P$ & Increase HBA

User: Can you make molecule `SMILES`less soluble in water and more hydrogen bond acceptors? The output molecule should be similar to the input molecule.
Output: One valid SMILES.

Prompt 203: Reduce $\log P$ & Increase HBD

User: Can you make molecule `SMILES`more soluble in water and more hydrogen bond donors? The output molecule should be similar to the input molecule.
Output: One valid SMILES.

Prompt 204: Increase $\log P$ & Increase HBD

User: Can you make molecule `SMILES`less soluble in water and more hydrogen bond donors? The output molecule should be similar to the input molecule.
Output: One valid SMILES.

Prompt 205: Reduce $\log P$ & Decrease TPSA

User: Can you make molecule `SMILES`more soluble in water and higher permeability? The output molecule should be similar to the input molecule.
Output: One valid SMILES.

Prompt 206: Reduce $\log P$ & Increase TPSA

User: Can you make molecule `SMILES`more soluble in water and lower permeability? The output molecule should be similar to the input molecule.
Output: One valid SMILES.

B SUPERVISED FINE-TUNING (SFT) DETAILS

For all our fine-tuning experiments, we utilize a memory-efficient, 4-bit quantized LLaMA 3.1 8B Instruct model as the backbone. Our datasets are consistently formatted as prompt-completion pairs, where the prompts are detailed in the main text and the corresponding completions are the child SMILES.

To ensure a fair comparison across benchmarks, we trained three models, as detailed in Table 2, each on a different dataset that has been filtered to contain comparable tasks. For the MEGA dataset, we retain tasks 101, 102, 103, 104, 107, and 108, resulting in 229K prompt-completion pairs. For MolEdit-Instruct, we use tasks 103, 104, 107, and 108 (as tasks 101 and 102 are not available), yielding 650K prompt-completion pairs. For MolOpt-Instructions, we include tasks 101, 102, 103, 104, 107, and 108, producing 301K prompt-completion pairs.

All models are trained using Low-Rank Adaptation (LoRA) with a rank of r=32 and α=16, targeting all attention projection matrices and feed-forward layers. We use a training batch size of 16 with a gradient accumulation of 2 steps, resulting in an effective batch size of 32. Optimization is performed with an 8-bit quantized AdamW optimizer for memory efficiency. The learning rate is set to $1e-4$ with a cosine annealing scheduler and a linear warm-up period of 100 steps. For regularization, a weight decay of 0.01 is applied. All models are trained with a maximum sequence length of 512 tokens, using mixed-precision training (bfloat16) when supported. All trainings are conducted on a single A100 (40GB) GPU for approximately 23 hours.

B.1 EVALUATION

We perform a sanity check to ensure that test SMILES are not present in any of the training sets using canonical SMILES notation to prevent any data leakage. Importantly, to ensure the fairest possible evaluation, we evaluate each model using the prompt templates specific to their respective training datasets. This means models trained on MolEdit-Instruct data are evaluated with MolEdit-Instruct prompt templates, while models trained on MEGA use MEGA templates, and models trained on MolOpt-Instructions use MolOpt-Instructions templates, eliminating any potential bias from prompt format differences.

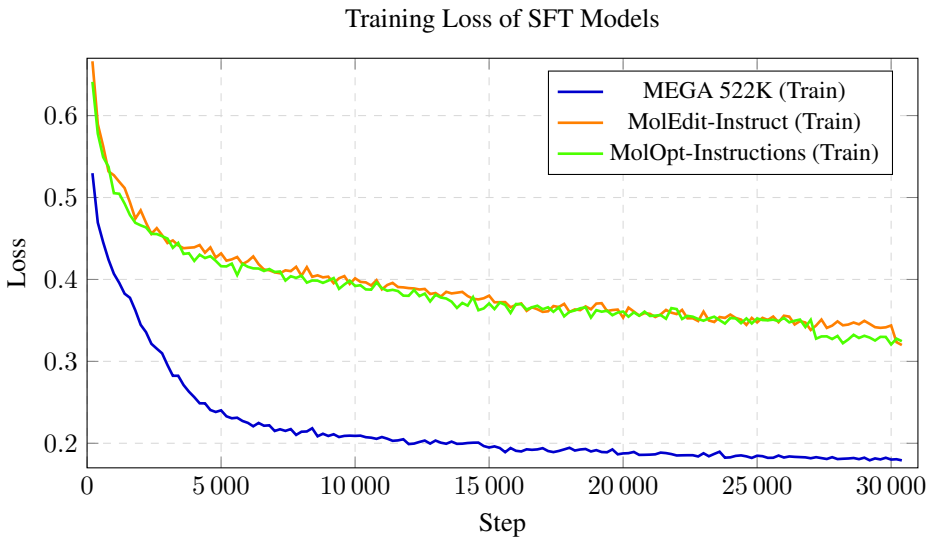

Figure 6: Training loss curves for three SFT models on MEGA, MolEdit-Instruct, and MolOpt-Instructions. MEGA achieves the lowest final loss ($\sim$0.18), followed by MolOpt-Instructions and MolEdit-Instruct respectively.

As shown in Figure 6 the model trained on MEGA exhibits significantly faster convergence and substantially lower final loss values. The better training dynamics observed with MEGA indicates that our dataset leads to more sample-efficient learning, achieving better optimization faster.

In addition, for Table 3, we report hit ratio results comparing MEGA GRPO against Gemini 2.5 Pro (June 17, 2025 official API release) and DrugAssist on the 500 test SMILES provided by DrugAssist.
This evaluation is performed over a single run, and we carefully verify that none of these 500 SMILES are included in our training set to avoid any possibility of data contamination.

B.2 Extra Comparisons

To further assess the utility of the MEGA dataset and extend the results in Table 2, we conducted an pair-wise comparison between MEGA and each external dataset on their overlapping task sets. Specifically, MEGA shares five tasks with MolEdit-Instruct and six with MolOpt-Instructions.

In the first experience, we trained models exclusively on the five tasks shared between MEGA and MolEdit-Instruct, namely tasks 103, 104, 107, 108, and 201 (Table 12). This setting corresponds to 678K training examples from MolEdit-Instruct and 183K examples from MEGA restricted to these five tasks. In the second, we trained models on the six tasks shared between MEGA and MolOpt-Instructions, namely tasks 101, 102, 103, 104, 107, and 108 (Table 13), which amounts to 301K training examples from MolOpt-Instructions and 229K examples from MEGA. All training hyperparameters and conditions described in Appendix B were kept identical to ensure a fair and controlled comparison.

In these head-to-head evaluations, we found that models trained on the MEGA data partitions, in average, outperform those trained on the corresponding data from MolEdit-Instruct and MolOpt-Instructions. This finding further validates the quality and effectiveness of our dataset, demonstrating that its superior performance is not limited to a small task intersection, but holds true in expanded comparisons.

Table 12: Performance comparison: MEGA vs MolEdit Instruct

Task	Threshold	MolEdit-Instruct	MEGA
103	0.0	27.19 ± 0.84	**61.05 ± 2.88**
	0.1	14.37 ± 0.95	**24.36 ± 1.73**
104	0.0	**99.28 ± 0.52**	95.84 ± 0.89
	0.1	**97.94 ± 0.55**	80.95 ± 3.41
107	0.0	95.72 ± 0.61	**98.02 ± 0.90**
	1.0	43.05 ± 1.64	**94.58 ± 0.76**
108	0.0	98.10 ± 0.71	**99.80 ± 0.25**
	1.0	66.53 ± 2.05	**97.25 ± 0.60**
201	0.0	87.14 ± 1.99	**96.18 ± 1.03**
	0.5	81.66 ± 1.72	**87.86 ± 1.58**
Average		71.10	**83.59**

Table 13: Performance comparison: MEGA vs MolOpt-Instructions

Task	Threshold	MolOpt-Instruction	MEGA
101	0.0	96.71 ± 0.70	**98.04 ± 0.51**
	0.5	**96.41 ± 0.58**	92.47 ± 0.79
102	0.0	88.41 ± 1.85	**97.41 ± 0.74**
	0.5	88.41 ± 1.85	**92.53 ± 2.25**
103	0.0	16.82 ± 1.57	**59.71 ± 1.29**
	0.1	8.68 ± 1.16	**26.72 ± 2.31**
104	0.0	**97.92 ± 1.40**	97.42 ± 0.32
	0.1	**93.68 ± 1.88**	84.54 ± 2.15
107	0.0	92.33 ± 2.42	**98.35 ± 0.50**
	1.0	33.41 ± 3.03	**93.36 ± 0.57**
108	0.0	94.76 ± 0.91	**100.00 ± 0.00**
	1.0	56.10 ± 1.74	**98.56 ± 0.89**
Average		71.97	**86.59**

C GRPO DETAILS

C.1 GRPO ALGORITHM FOR MOLECULAR EDITING

For each molecular editing prompt (x_{in}, x_t), GRPO operates as follows:

1. **Sample a group of candidate molecules**:
$$\{y_1, y_2, ..., y_G\} \sim \pi_\theta(\cdot|x_{\text{in}}, x_t) \tag{1}$$
where G is the number of generations by our policy model
2. **Compute rewards for all candidates** using batch molecular property evaluation:
$$r_i = R(y_i, x_{\text{in}}, x_t) \quad \text{for } i = 1, ..., G \tag{2}$$
3. **Calculate group-relative advantages**:
$$\hat{A}_i = \frac{r_i - \bar{r}}{\sigma_r + \epsilon} \tag{3}$$
where $\bar{r} = \frac{1}{G}\sum_{j=1}^{G} r_j$ and $\sigma_r = \sqrt{\frac{1}{G}\sum_{j=1}^{G}(r_j - \bar{r})^2}$ are the mean and standard deviation of rewards within the group, and $\epsilon = 10^{-8}$ for numerical stability.
4. **Update the policy** using the GRPO objective:
$$\mathcal{L}_{\text{GRPO}}(\theta) = -\frac{1}{\sum_{i=1}^{G}|y_i|}\sum_{i=1}^{G}\sum_{t=1}^{|y_i|}\left[\min\left(\rho_{i,t}\hat{A}_i, \text{clip}(\rho_{i,t}, 1-\varepsilon, 1+\varepsilon)\hat{A}_i\right) - \beta D_{\text{KL}}[\pi_\theta \| \pi_{\text{ref}}]\right] \tag{4}$$
where:
   - $\rho_{i,t} = \frac{\pi_\theta(y_{i,t}|x_{\text{in}}, x_t, y_{i,<t})}{\pi_{\theta_{\text{old}}}(y_{i,t}|x_{\text{in}}, x_t, y_{i,<t})}$ is the probability ratio
   - $\varepsilon = 0.2$ is the clipping parameter
   - $\beta = 0.0$ by default
   - If $\beta > 0$, the KL divergence is estimated as shown previously

C.2 EXPERIMENTAL DETAILS

For locality-aware GRPO training, we ensured strict consistency between supervised fine-tuning (SFT) and post-training data. For example, the MEGA GRPO (14K) model used the same 14K SMILES for both SFT and GRPO. Similarly, the results in Table 4 were obtained from a policy model first fine-tuned on the full 522K prompt–completion pairs of MEGA, with the same data reused during GRPO. In this phase, we sampled $G = 12$ generations per prompt and computed rewards for each candidate molecule.

Our composite reward function is designed to guide the model toward valid, improved, and structurally related molecules using three distinct signals. First, the validity reward provides a binary signal that ensures chemical correctness through RDKit sanitization while rejecting any outputs that are unchanged or fragmented. Second, the property reward implements a task-specific evaluation using a dual-threshold mechanism to provide fine-grained control over property modifications. Strict thresholds (e.g., ΔLogP > 0.5, ΔQED > 0.1) yield a reward of 1.0, whereas loose thresholds that only require a correct directional change yield 0.5. This encourages the model to learn both conservative and substantial improvements. Third, the Tanimoto similarity reward enforces structural conservation, assigning a reward of 1.0 for high similarity (Tanimoto coefficient > 0.65), 0.5 for moderate modifications (coefficients $\in$ [0.4, 0.65]), and 0.0 for major scaffold modifications (coefficients < 0.4).

All GRPO training was conducted on a single A100 GPU, with convergence achieved in approximately 10 hours at around 3,000 steps. We used an 8-bit quantized AdamW optimizer with a learning rate of $\alpha = 5 \times 10^{-6}$, $\beta_1 = 0.9$, $\beta_2 = 0.999$, a weight decay of 0.01, and gradient norm clipping at 0.5. The learning rate followed a cosine annealing schedule with a 10% linear warmup. To ensure memory efficiency, the model incorporated 4-bit quantization and LoRA adaptation with a rank of $r = 32$. We used an effective batch size of 8 (4 samples per device with 2 gradient accumulation steps) and maximum sequence lengths of 256 and 128 for prompts and completions, respectively. All computations were performed using bfloat16 mixed precision.

D IMPACT OF GRPO AND TANIMOTO REWARD ON SCAFFOLD SIMILARITY

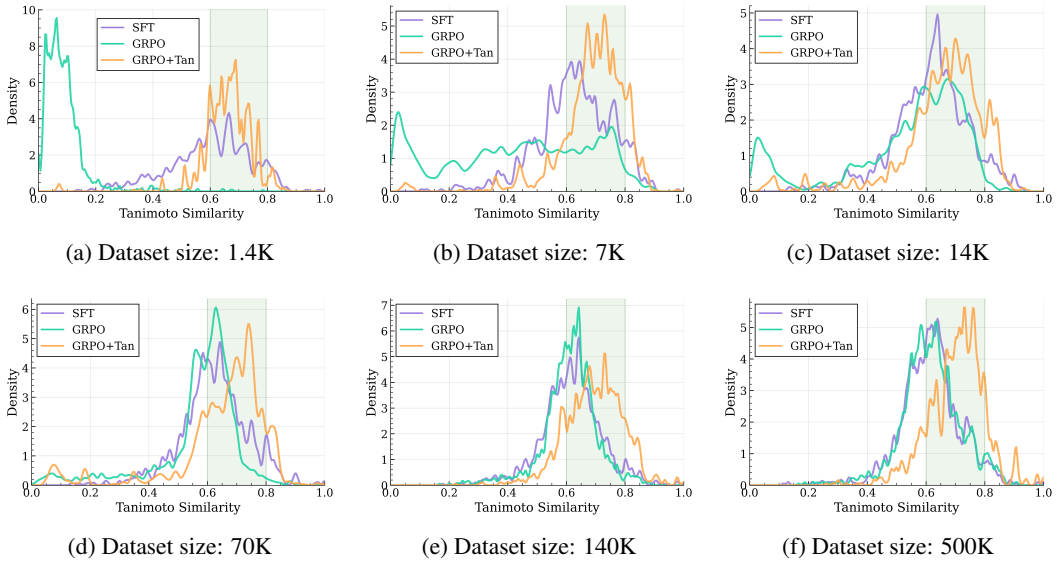

(a) Dataset size: 1.4K (b) Dataset size: 7K (c) Dataset size: 14K

(d) Dataset size: 70K (e) Dataset size: 140K (f) Dataset size: 500K

Figure 7: Tanimoto similarity distributions for different training data sizes. Each plot shows the distribution for SFT (purple), GRPO without Tanimoto reward (turquoise), and GRPO with Tanimoto reward (orange) models. The green shaded region (0.6–0.8) indicates the targeted tanimoto similarity range.

Figure 7 shows the results of LLM postraining across varying dataset sizes sampled from MEGA using GRPO with and without incorporating a Tanimoto similarity component into the reward system. When trained without the Tanimoto reward on small datasets, the models achieve high hit ratios but tend to alter the scaffold substantially, yielding molecules with low similarity to their parent compounds. As the dataset size increases, however, the model implicitly recovers the similarity distribution observed in the SFT baseline, ultimately reaching the target similarity regime even without an explicit reward signal. In contrast, when the Tanimoto reward is included, the model attains this small-edit regime with as few as 1.4k training examples (roughly 100 per task type).

E QUALITATIVE EXAMPLES

Table 14: Visualization of molecular editing with three actions: Replace, Insert, and Delete. The yellow regions indicate replaced substructures, the blue regions indicate inserted substructures, and the red regions indicate deleted substructures. Each example shows the transformation from the input molecule $\mathbf{x}_{\text{in}}$ to the output molecule $\mathbf{x}_{\text{out}}$.

(a) 101 (strict) (b) 106 (strict)
Input Molecule $\mathbf{x}_{\text{in}} \rightarrow$ Output Molecule $\mathbf{x}_{\text{out}}$ Input Molecule $\mathbf{x}_{\text{in}} \rightarrow$ Output Molecule $\mathbf{x}_{\text{out}}$
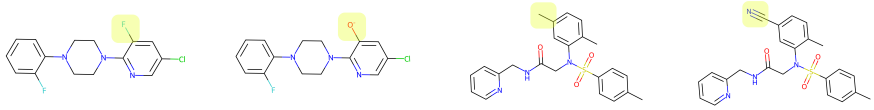 LogP: 3.3398 $\rightarrow$ 2.2743 TPSA: 79.3700 $\rightarrow$ 103.1600
(c) 102 (strict) (d) 103 (loose)
Input Molecule $\mathbf{x}_{\text{in}} \rightarrow$ Output Molecule $\mathbf{x}_{\text{out}}$ Input Molecule $\mathbf{x}_{\text{in}} \rightarrow$ Output Molecule $\mathbf{x}_{\text{out}}$
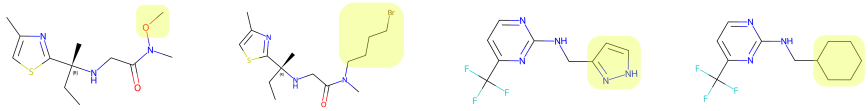 LogP: 1.6861 $\rightarrow$ 3.2998 QED: 0.8626 $\rightarrow$ 0.9025
(e) 105 (strict) (f) 107 (loose)
Input Molecule $\mathbf{x}_{\text{in}} \rightarrow$ Output Molecule $\mathbf{x}_{\text{out}}$ Input Molecule $\mathbf{x}_{\text{in}} \rightarrow$ Output Molecule $\mathbf{x}_{\text{out}}$
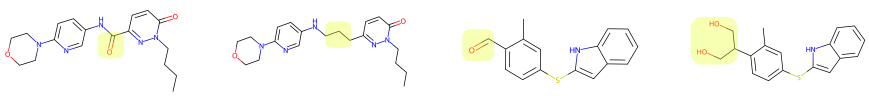 TPSA: 89.3500 $\rightarrow$ 72.2800 H-Bond Acceptors: 2 $\rightarrow$ 3
(g) 108 (strict) (h) 205 (strict)
Input Molecule $\mathbf{x}_{\text{in}} \rightarrow$ Output Molecule $\mathbf{x}_{\text{out}}$ Input Molecule $\mathbf{x}_{\text{in}} \rightarrow$ Output Molecule $\mathbf{x}_{\text{out}}$
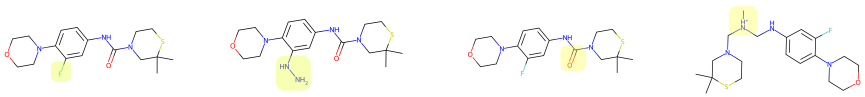 H-Bond Donors: 1 $\rightarrow$ 3 LogP: 3.0216 $\rightarrow$ 1.3313, TPSA: 44.81 $\rightarrow$ 32.18

(i) 101 (strict) (j) 102 (strict)

Input Molecule $\mathbf{x}_{\text{in}} \rightarrow$ Output Molecule $\mathbf{x}_{\text{out}}$ Input Molecule $\mathbf{x}_{\text{in}} \rightarrow$ Output Molecule $\mathbf{x}_{\text{out}}$

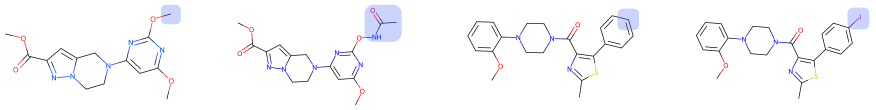

LogP: 0.4971 → -0.0816 LogP: 4.0895 → 4.6941

(k) 104 (strict) (l) 201 (strict)

Input Molecule $\mathbf{x}_{\text{in}} \rightarrow$ Output Molecule $\mathbf{x}_{\text{out}}$ Input Molecule $\mathbf{x}_{\text{in}} \rightarrow$ Output Molecule $\mathbf{x}_{\text{out}}$

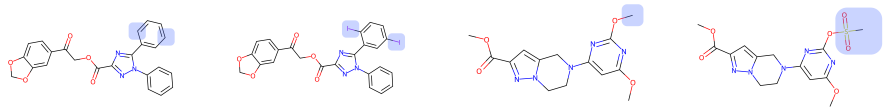

QED: 0.3421 → 0.1626 LogP: 0.4971 → -0.1731, H-Acceptors: 9 → 11

(m) 202 (strict) (n) 204 (strict)

Input Molecule $\mathbf{x}_{\text{in}} \rightarrow$ Output Molecule $\mathbf{x}_{\text{out}}$ Input Molecule $\mathbf{x}_{\text{in}} \rightarrow$ Output Molecule $\mathbf{x}_{\text{out}}$

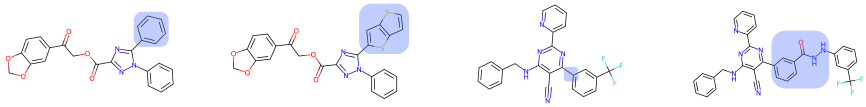

LogP: 3.7027 → 4.9789, H-Acceptors: 8 → 10 LogP: 5.7082 → 6.4651, H-Donors: 1 → 3

(o) 206 (strict) (p) 108 (strict)

Input Molecule $\mathbf{x}_{\text{in}} \rightarrow$ Output Molecule $\mathbf{x}_{\text{out}}$ Input Molecule $\mathbf{x}_{\text{in}} \rightarrow$ Output Molecule $\mathbf{x}_{\text{out}}$

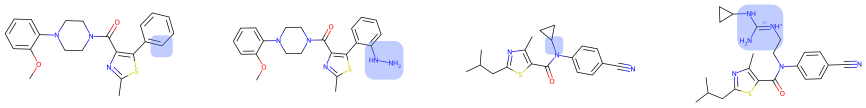

LogP: 4.0895 → 3.3751, TPSA: 45.67 → 83.72 H-Bond Donors: 0 → 3

(q) 102 (strict) (r) 103 (strict)

Input Molecule $\mathbf{x}_{\text{in}} \rightarrow$ Output Molecule $\mathbf{x}_{\text{out}}$ Input Molecule $\mathbf{x}_{\text{in}} \rightarrow$ Output Molecule $\mathbf{x}_{\text{out}}$

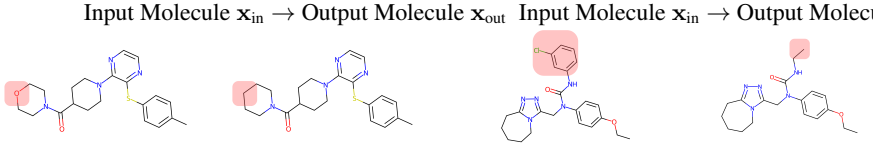

LogP: 3.0114 → 3.5138 QED: 0.5656 → 0.8620

(s) 105 (strict) (t) 105 (strict)

Input Molecule $\mathbf{x}_{\text{in}} \rightarrow$ Output Molecule $\mathbf{x}_{\text{out}}$ Input Molecule $\mathbf{x}_{\text{in}} \rightarrow$ Output Molecule $\mathbf{x}_{\text{out}}$

TPSA: 31.3500 → 18.4600 TPSA: 55.4000 → 38.3300

F Dataset License

We derived our work from the ZINC 250K dataset Akhmetshin et al. (2021), available here , which is distributed under the GNU General Public License v3 or later (GPL-3.0+). In accordance with this license, we release our derived dataset under the same terms, preserving the freedoms to use, share, and modify the data.